Demonstration of AlN Schottky Barrier Diodes With Blocking Voltage Over 1 kV

Houqiang Fu, Izak Baranowski, Xuanqi Huang, Hong Chen, Zhijian Lu, Jossue Montes, Xiaodong Zhang, and Yuji Zhao, *Member, IEEE*

***Abstract*— This letter reports the first demonstration of 1-kV-class AlN Schottky barrier diodes on sapphire substrates by metal organic chemical vapor deposition. The device structure mimics the silicon-on-insulator (SOI) technology, consisting of thin n-AlN epilayer as the device active region and thick resistive AlN underlayer as the insulator. At room temperature, the devices show outstanding performances with a low turn-ON voltage of 1.2 V, a high ON/OFF ratio of ~10^5, a low ideality factor of 5.5, and a low reverse leakage current below 1 nA. The devices also exhibit excellent thermal stability over 500 K owing to the ultra-wide bandgap of AlN. The breakdown voltage of the devices can be further improved by employing field plate, edge termination technologies, and optimizing the SOI-like device structure. This letter presents a cost-effective route to high performance AlN-based Schottky barrier diodes for high-power, high-voltage, and high-temperature applications.**

***Index Terms*— Aluminum nitride, Schottky barrier diodes, power electronics, high temperature, semiconductor, breakdown.**

I. Introduction

WURTZITE AlN has the largest bandgap of 6.2 eV among the wide bandgap semiconductor family including SiC (3.3 eV), GaN (3.4 eV), β-Ga_2O_3 (4.8 eV) and diamond (5.5 eV), which are attractive for various optoelectronic and electronic applications. Currently, AlN primarily serves as substrates or templates on which devices are grown, while its III-nitride counterparts [i.e., In(Ga)N and Ga(Al)N], have been widely utilized as device active regions [1]–[13]. For example, ultraviolet (UV) light emitting diodes (LEDs) [14], [15] and various field-effect transistors (FETs) [16]–[19] have been demonstrated on AlN substrates or templates. For power electronics, AlN devices have the potential to outperform current GaN devices due to AlN's larger critical electric field (12 MV/cm) and thermal conductivity (340 W/mK). However, due to the challenges in material growth and device fabrication, very limited work has been reported on AlN electronics. Reddy *et al.* [20] investigated the Schottky barrier heights between AlN and different metals. Irokawa *et al.* [21] first demonstrated AlN based lateral Schottky barrier diodes (SBDs) directly on unintentionally doped (UID) AlN substrate grown by physical vapor transport (PVT). The n-type conductivity was thought to originate from unintentional oxygen impurities or nitrogen vacancies. Their devices exhibited a turn-on voltage of 2.6 V, an ideality factor of 12, and a breakdown voltage below 50 V. Kinoshita *et al.* [22] fabricated a vertical AlN SBD on 250-μm-thick n-AlN substrate by hydride phase vapor epitaxy (HVPE) after removing the insulating seed substrate. However, the removal process caused a significant amount of surface damages, which led to lower device performances compared with theoretical results. The AlN SBD had a turn-on voltage of 2.2 V, an ideality factor of 8, and a breakdown voltage of 550−770 V. The breakdown voltage of the devices could be enhanced by implementing field plates [23], edge terminations [10], and material improvements such as reducing defect density [9]. However, bulk AlN substrates are still too expensive and highly doped n-AlN substrates are not readily available, rendering lateral and vertical AlN SBDs on AlN substrates not commercially attractive or research-friendly. Recently, AlN epilayers with high crystal quality were achieved using metal organic chemical vapor deposition (MOCVD) on sapphire substrates [24]–[26], which opens the door to cost-effective high-performance AlN electronic devices. In this work, we demonstrated, for the first time, high performance AlN SBDs on sapphire substrates with a low turn-on voltage of 1.2 V, a high on/off ratio of ~10^5, a low ideality factor of 5.5 and a high breakdown voltage over 1 kV.

II. Growth, Material Characterization and Device Fabrication

The AlN SBDs epilayers were grown by MOCVD on single side polished (SSP) (0001) sapphire substrate with 0.2° off-cut angle. The Al and N sources were trimethylaluminum (TMAl) and ammonia (NH_3), respectively. SiH_4 was used as the precursor for n-type dopant Si. The carrier gas was hydrogen (H_2). The details about the growth can be found elsewhere [25]. The device structure (Fig. 1) consists of a AlN buffer layer, an 1-μm-thick resistive UID AlN underlayer (UL), a 300 nm Si-doped n-AlN layer and a 2 nm UID GaN capping layer. The thin UID GaN capping layer was used to prevent the oxidation of AlN epilayers underneath that might degrade the device performances [17]. The crystal quality of the MOCVD AlN sample was characterized by high resolution X-ray diffraction (HRXRD) measurement using PANalytical X'Pert Pro materials research X-ray diffractometer (MRD) system with Cu Kα radiations. Hybrid monochromator and triple axis module are used for the incident and diffracted

Manuscript received June 13, 2017; revised June 24, 2017; accepted July 2, 2017. Date of publication July 5, 2017; date of current version August 23, 2017. This work was supported by the Defense Threat Reduction Agency Young Investigator Award. The review of this letter was arranged by Editor T. Palacios. *(Corresponding author: Yuji Zhao.)*

The authors are with the School of Electrical, Computer, and Energy Engineering, Arizona State University, Tempe, AZ 85287 USA (e-mail: yuji.zhao@asu.edu).

Color versions of one or more of the figures in this letter are available online at http://ieeexplore.ieee.org.

Digital Object Identifier 10.1109/LED.2017.2723603

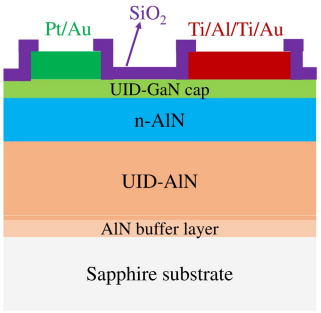

Fig. 1. Schematic view of fabricated AlN SBDs on sapphire by MOCVD. The ohmic and Schottky contacts are in red and green, respectively.

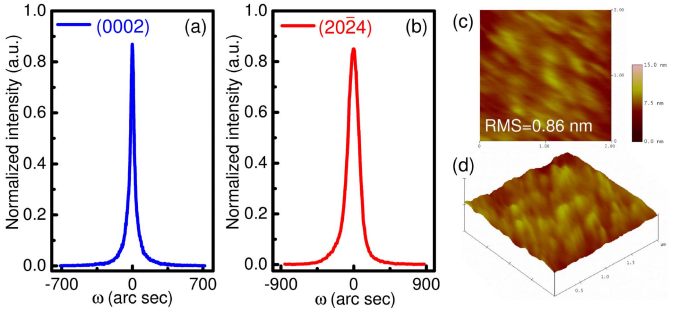

Fig. 2. Rocking curve of (a) (0002) plane and (b) (20$\bar{2}$4) for AlN SBDs by HRXRD. AFM images in (c) two dimension and (d) three dimension.

beam optics, respectively. Figure 2(a) and 2(b) show the (0002) symmetric and (20$\bar{2}$4) asymmetric plane rocking curves (RCs) for the AlN sample. The full width at half maximum (FWHM) of (0002) RC are 46.8 arc sec and FWHM of (20$\bar{2}$4) RC are 159.1 arc sec, which are among the lowest FWHM reported on MOCVD grown AlN epilayers on sapphire substrate [25], [26]. The dislocation density of the sample was estimated to be $\sim 10^8$ cm^{-2} using the equations in Ref. 27. The surface morphology of the AlN sample was examined by Bruker's Dimension atomic force microscopy (AFM). The root-mean-square (RMS) roughness of 2×2 μm^2 scanning area of the samples was measured to be 0.86 nm. The HRXRD and AFM results show AlN epilayers with low defect density and good surface morphology were obtained on sapphire substrates.

The as-grown sample was cleaned in acetone and isopropyl alcohol under ultrasonic and dipped in hydrochloric acid (HCl : H_2O = 1:2) before the metal depositions. The AlN SBD devices were fabricated using conventional optical photolithography and lift-off processes. For the ohmic contacts, Ti/Al/Ti/Au (20 nm / 100 nm / 20 nm / 50 nm) metal stacks were deposited by electron beam deposition followed by thermal annealing at 1000 °C in nitrogen for 30 seconds using rapid thermal annealing (RTA). The circular ohmic contact has a diameter of 400 μm. For the Schottky contacts, Pt/Au (30 nm / 120 nm) metal stacks were deposited by electron beam evaporation. For comparison, both circular (diameter of 100 μm) and square Schottky contacts (side length of 100 μm) were fabricated. The distance between the ohmic contact and Schottky contact is 200 μm. A 200 nm SiO_2 passivation layer was then deposited on the devices using plasma-enhanced chemical vapor deposition (PECVD) at 350 °C and 1000 mTorr with a RF power of 20 W. Finally, the contact vias were opened by fluorine-based reactive ion

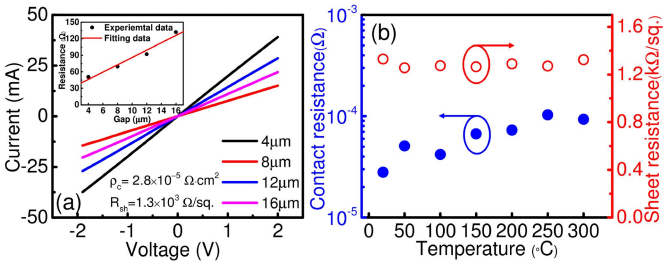

Fig. 3. (a) TLM I–V characteristics of the ohmic contact at RT. The inset shows the resistance versus gap of the TLM pads. A linear fitting was performed to extract the contact resistance and sheet resistance. (b) Contact resistance and sheet resistance as a function of temperature.

etching (RIE). No field plate or edge termination were implemented in the devices. The ohmic contacts of the devices were investigated by transmission line method (TLM) from room temperature (RT) to 300 °C. Figure 3(a) shows the TLM current–voltage (I–V) curves at RT. The contacts showed good ohmic behavior with a contact resistance of 2.8×10^{-5} Ω·cm^2 and a sheet resistance of 1.3×10^3 Ω/sq. The ohmic contacts also exhibited excellent thermal stability over the measured temperature range (RT to 300 °C). The contact resistance slightly increased with the increasing temperature. This was not necessarily the intrinsic nature of the ohmic contact of AlN because stressful probes could destroy the integrity of metal stacks and thus resulted in somehow a degradation of ohmic contacts [28]. The physical mechanism is still unclear and demands further investigations. The electrical measurements were conducted on a probe station equipped with a thermal chuck. The I–V characteristics at forward bias and reverse bias were measured using the Keithley 2410 sourcemeter. The capacitance-voltage (C–V) characteristics were measured with the Keithley 4200-SCS parameter analyzer. The reverse breakdown measurements were performed in insulating Fluorinert liquid FC-70 at RT.

III. Results and Discussions

Figure 4(a) shows the temperature-dependent forward I–V characteristics of the circular AlN SBDs. The lower current detection limit of the setup is 1 nA. The measured off current densities were as low as $\sim10^{-6}$ A/cm^2 at all temperatures. A high on/off ratio $\sim10^5$ was obtained, which is comparable to that of AlN SBDs on AlN substrates [21], [22]. The turn-on voltage of the devices was 1.2 V (1.1 V for square SBDs), smaller than previous reported values [21], [22]. The constant slope of Richardson plot (J/T^2 vs. 1/kT where J is the current density, k is the Boltzmann constant and T is the temperature) in Fig. 4(b), indicated the forward current of the devices was limited by thermionic emission [29], [30].

The general diode equations for thermionic emission can be expressed as [22], [31]

$$J = J_0 \exp(q(V - IR_s)/nkT - 1) \quad (1)$$

$$J_0 = A^*T^2 \exp(-\Phi_B/kT) \quad (2)$$

where J_0 is the saturation current density, R_s is the series resistance, n is the ideality factor, $A*$ is the Richardson constant and $\hat{O}_B$ is the barrier height. The Richardson constant was calculated to be 48 A/(cm^2 K^2) using the effective electron mass of 0.5 m$_0$ [22]. Based on Eqs. (1) and (2), ideality

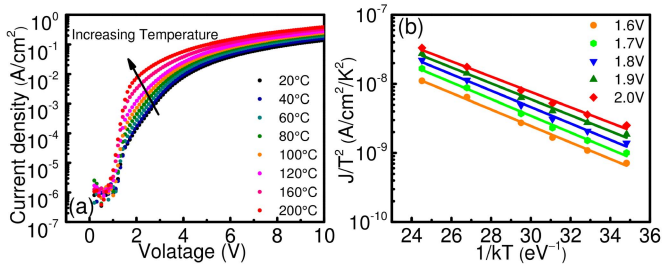

Fig. 4. (a) Forward I–V characteristics of the AlN SBD from 20 °C to 200 °C. (b) The Richardson plot from 1.6V to 2.0 V in a step of 0.1 V.

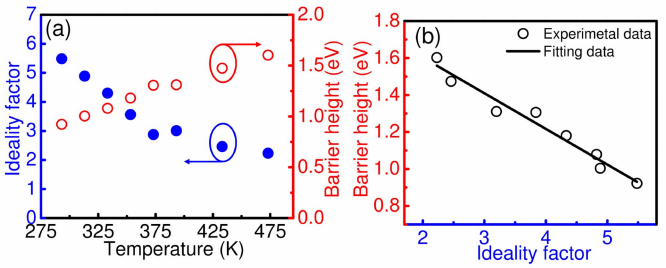

Fig. 5. (a) Ideality factor and barrier height as a function of temperature. (b) Barrier height vs. ideality factor.

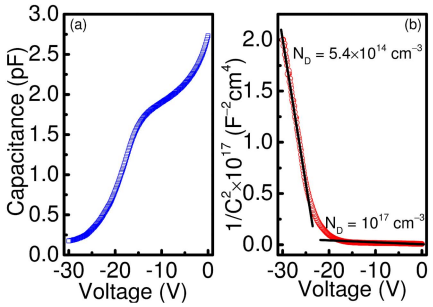

Fig. 6. (a) C-V and (b) $1/C^2$ vs. V characteristics for AlN SBDs at 1 MHz. The doping concentrations of are extracted from the slopes in $1/C^2$ vs. V

factor and barrier height of the AlN SBDs were extracted as a function of temperature in Fig. 5(a). The ideality factor decreased from 5.5 to 2.2 while the barrier height increased from 0.9 eV to 1.6 eV from 20 °C to 200 °C. The temperature dependence of the ideality factor was attributed to the lateral inhomogeneity of the Schottky barrier interface [21]. Note that the RT ideality factors (n = 5.5 and 5.3 for circular and square SBDs, respectively) obtained in this work were 2∼3 times smaller than previous results [21], [22], possibly due to improved material quality and metal/semiconductor interface. A well-known linear correlation between the barrier height and the ideality factor was also observed due to the nonuniform Schottky interface [31]. It should be noted that the thin GaN capping layer did not contribute to the device operation under bias.

Figure 6(a) shows C–V characteristics of the AlN SBDs at a frequency of 1 MHz. The net doping concentration N_D can be obtained using [29]

$$1/C^2 = \frac{2}{q\varepsilon_0\varepsilon_r N_D}(V_{bi} - V - kT/q) \quad (3)$$

$$d\left(1/C^2\right)/dV = -\frac{2}{q\varepsilon_0\varepsilon_r N_D} \quad (4)$$

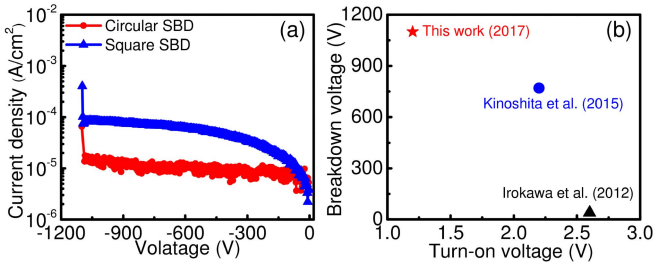

Fig. 7. (a) Reverse I-V characteristics of circular and square AlN SBDs. (b) Comparison of the breakdown and turn-on voltages of reported AlN SBDs.

where V_{bi} is the built-in voltage, ε_0 is permittivity of the vacuum, and ε_r is relative permittivity of AlN. After plotting $1/C^2$ vs. V, two slopes were observed, which corresponded to the net doping concentrations in n-AlN layer ($N_D = 10^{17}$ cm^{-3}) and resistive UID AlN UL ($N_D = 5.4 \times 10^{14}$ cm^{-3}), respectively. This result indicated UID AlN UL was much more resistive than n-AlN layer. The high resistivity of UID AlN UL was also confirmed by the contactless sheet resistance measurement using Model LEI-88, exceeding the apparatus upper limit of 10^4 Ω/sq. . The Silvaco ATLAS simulation showed the majority of current paths were confined in the thin n-AlN layer due to the high resistivity of UID AlN UL. Therefore, growing thick resistive UID AlN UL can not only improve the material quality of n-AlN epilayer, but may also reduce the current leakage and increase the breakdown voltage, similar to the SOI technology.

Figure 7(a) presents the reverse I–V characteristics of the circular and square AlN SBDs. Both devices exhibited breakdown voltages over 1 kV, which are much higher than previous reports (∼ 700 V) [22]. The catastrophic damages of the AlN SBDs occurred at the edge of Schottky contacts due to edge electric field crowding. The breakdown was therefore not intrinsically limited by the critical electric field of AlN. Improvement in the breakdown capability of the devices can be further expected by employing field plate and/or edge termination. In addition, improving the material quality of n-AlN, increasing the resistivity of the UID AlN UL by Fe or C doping and optimizing the passivation strategies can also help to increase the breakdown voltage of the devices.

IV. Conclusion

In summary, lateral AlN SBDs were grown and fabricated on sapphire substrates by MOCVD. At forward bias, the AlN SBDs exhibit good rectifying behavior with a turn-on voltage of 1.2 V, an on/off ratio of ∼ 10^5, and an ideality factor of 5.5 at RT. At reverse bias, the devices demonstrated over 1 kV breakdown voltage and below 1 nA leakage current. Material growth and device structure optimizations are expected to further increase the breakdown voltage. In addition, the devices show excellent thermal stability over 500 K. These results showed high potential of AlN SBDs on sapphire substrate for high power, high voltage and high temperature applications.

Acknowledgment

The samples were provided by Kyma Technologies. The authors gratefully acknowledge the use of facilities within the LeRoy Eyring Center for Solid State Science at Arizona State University.

REFERENCES

[1] S. Nakamura, G. Fasol, and S. J. Pearton, *The Blue Laser Diode: The Complete Story*, 2nd ed. Berlin, Germany: Springer, 2000, doi: 10.1007/978-3-662-04156-7.

[2] C. C. Pan, Q. Yan, H. Fu, Y. Zhao, Y. R. Wu, C. G. Van de Walle, S. Nakamura, and S. P. DenBaars, "High optical power and low efficiency droop blue light-emitting diodes using compositionally step-graded InGaN barrier," *Electron. Lett.*, vol. 51, no. 15, pp. 1187–1189, Jul. 2015, doi: 10.1049/el.2015.1647.

[3] H. Fu, Z. Lu, X. Zhao, Y. Zhang, S. P. DenBaars, S. Nakamura, and Y. Zhao, "Study of low efficiency droop in semipolar (20-2-1) InGaN light-emitting diodes by time-resolved photoluminescence," *J. Display Technol.*, vol. 12, no. 7, pp. 736–741, Jul. 2016, doi: 10.1109/JDT.2016.2521618.

[4] H. Chen, H. Fu, Z. Lu, X. Huang, and Y. Zhao, "Optical properties of highly polarized InGaN light-emitting diodes modified by plasmonic metallic grating," *Opt. Exp.*, vol. 24, no. 10, pp. A856–A867, Apr. 2016, doi: 10.1364/OE.24.00A856.

[5] X. Huang, H. Fu, H. Chen, Z. Lu, D. Ding, and Y. Zhao, "Analysis of loss mechanisms in InGaN solar cells using a semi-analytical model," *J. Appl. Phys.*, vol. 119, no. 21, p. 213101, Jun. 2016, doi: 10.1063/1.4953006.

[6] H. Fu, H. Chen, X. Huang, Z. Lu, and Y. Zhao, "Theoretical analysis of modulation doping effects on intersubband transition properties of semipolar AlGaN/GaN quantum well," *J. Appl. Phys.*, vol. 121, no. 1, p. 014501, Jan. 2017, doi: 10.1063/1.4972975.

[7] Y.-F. Wu, D. Kapolnek, J. P. Ibbetson, P. Parikh, B. P. Keller, and U. K. Mishra, "Very-high power density AlGaN/GaN HEMTs," *IEEE Trans. Electron Devices*, vol. 48, no. 3, pp. 586–590, Mar. 2001.

[8] K. Nomoto, B. Song, Z. Hu, M. Zhu, M. Qi, N. Kaneda, T. Mishima, T. Nakamura, D. Jena, and H. G. Xing, "1.7-kV and 0.55- mΩ·cm^2 GaN p-n diodes on bulk GaN substrates with avalanche capability," *IEEE Electron Device Lett.*, vol. 37, no. 2, pp. 161–164, Feb. 2016, doi: 10.1109/LED.2015.2506638.

[9] H. Fu, X. Huang, H. Chen, Z. Lu, X. Zhang, and Y. Zhao, "Effect of buffer layer design on vertical GaN-on-GaN p-n and Schottky power diodes," *IEEE Electron Device Lett.*, vol. 38, no. 6, pp. 763–766, Apr. 2017, doi: 10.1109/LED.2017.2690974.

[10] I. C. Kizilyalli, T. Prunty, and O. Aktas, "4-kV and 2.8- mΩ - cm^2 vertical GaN p-n diodes with low leakage currents," *IEEE Electron Device Lett.*, vol. 36, no. 10, pp. 1073–1075, Oct. 2015, doi: 10.1109/LED.2015.2474817.

[11] H. Fu, Z. Lu, X. Huang, H. Chen, and Y. Zhao, "Crystal orientation dependent intersubband transition in semipolar AlGaN/GaN single quantum well for optoelectronic applications," *J. Appl. Phys.*, vol. 119, no. 17, p. 174502, May 2016, doi: 10.1063/1.4948667.

[12] R. Chu, A. Corrion, M. Chen, R. Li, D. Wong, D. Zehnder, B. Hughes, and K. Boutros, "1200-V normally Off GaN-on-Si field-effect transistors with low dynamic on -resistance," *IEEE Electron Device Lett.*, vol. 32, no. 5, pp. 632–634, May 2011, doi: 10.1109/LED.2011.2118190.

[13] H. Fu, Z. Lu, and Y. Zhao, "Analysis of low efficiency droop of semipolar InGaN quantum well light-emitting diodes by modified rate equation with weak phase-space filling effect," *AIP Adv.*, vol. 6, no. 6, p. 065013, Jun. 2016, doi: 10.1063/1.4954296.

[14] T. Kinoshita, T. Obata, T. Nagashima, H. Yanagi, B. Moody, S. Mita, S. Inoue, Y. Kumagai, A. Koukitu, and Z. Sitar, "Performance and reliability of deep-ultraviolet light-emitting diodes fabricated on AlN substrates prepared by hydride vapor phase epitaxy," *Appl. Phys. Exp.*, vol. 6, no. 9, p. 092103, Aug. 2013, doi: 10.7567/APEX.6.092103.

[15] S. M. Islam, K. Lee, J. Verma, V. Protasenko, S. Rouvimov, S. Bharadwaj, H. Xing, and D. Jena, "MBE-grown 232-270 nm deep-UV LEDs using monolayer thin binary GaN/AlN quantum heterostructures," *Appl. Phys. Lett.*, vol. 110, no. 4, Jan. 2017, doi: 10.1063/1.4975068.

[16] M. Qi, G. Li, S. Ganguly, P. Zhao, X. Yan, J. Verma, B. Song, M. Zhu, K. Nomoto, H. Xing, and D. Jena, "Strained GaN quantum-well FETs on single crystal bulk AlN substrates," *Appl. Phys. Lett.*, vol. 110, no. 6, p. 063501, Feb. 2017, doi: 10.1063/1.4975702.

[17] G. Li, B. Song, S. Ganguly, M. Zhu, R. Wang, X. Yan, J. Verma, V. Protasenko, H. Xing, and D. Jena, "Two-dimensional electron gases in strained quantum wells for AlN/GaN/AlN double heterostructure field-effect transistors on AlN," *Appl. Phys. Lett.*, vol. 104, no. 19, p. 193506, May 2014, doi: 10.1063/1.4875916.

[18] G. Li, R. Wang, J. Guo, J. Verma, Z. Hu, Y. Yue, F. Faria, Y. Cao, M. Kelly, T. Kosel, H. G. Xing, and D. Jena, "Ultrathin body GaN-on-insulator quantum well FETs with regrown ohmic contacts," *IEEE Electron Device Lett.*, vol. 33, no. 5, pp. 661–663, May 2012.

[19] A. Baca, A. Armstrong, A. Allenman, E. Douglas, C. Sanchez, M. King, M. Coltrin, T. Fortune, and R. Kaplar, "An AlN/$Al_{0.85}Ga_{0.15}N$ high electron mobility transistor," *Appl. Phys. Lett.*, vol. 109, no. 3, p. 033509, Jul. 2016, doi: 10.1063/1.4959179.

[20] P. Reddy, I. Bryan, Z. Bryan, J. Tweedie, R. Kirste, R. Collazo, and Z. Sitar, "Schottky contact formation on polar and nonpolar AlN," *J. Appl. Phys.*, vol. 116, no. 19, p. 194503, Nov. 2014, doi: 10.1063/1.4901954.

[21] Y. Irokawa, E. Villora, and K. Shimamura, "Shottky Barrier Diodes on AlN Free-Standing Substrates," *Jpn. J. Appl. Phys.*, vol. 51, no. 4R, p. 040206, Mar. 2012, doi: 10.1143/JJAP.51.040206.

[22] T. Kinoshita, T. Nagashima, T. Obata, S. Takashima, R. Yamamoto, R. Togashi, Y. Kumagai, R. Schlesser, R. Collazo, A. Koukitu, and Z. Sitar, "Fabrication of vertical Schottky barrier diodes on n-type freestanding AlN substrates grown by hydride vapor phase epitaxy," *Appl. Phys. Exp.*, vol. 8, no. 6, p. 061003, May 2015, doi: 10.7567/APEX.8.061003.

[23] S. Rajabi, A. A. Orouji, H. A. Moghadam, S. E. J. Mahabadi, and M. Fathipour, "A novel double field-plate power high electron mobility transistor based on AlGaN/GaN for performance improvement," in *Proc. IEEE ICSCCN*, Jul. 2011, pp. 272–276, doi: 10.1109/ICSCCN.2011.6024558.

[24] Y. A. Xi, K. X. Chen, F. Mont, J. K. Kim, C. Wetzel, E. F. Schubert, W. Liu, X. Li, and J. A. Smart, "Very high quality AlN grown on (0001) sapphire by metal-organic vapor phase epitaxy," *Appl. Phys. Lett.*, vol. 89, no. 10, p. 103106, Sep. 2006, doi: 10.1063/1.2345256.

[25] T. Y. Wang, J. H. Liang, G. W. Fu, and D. S. Wuu, "Defect annihilation mechanism of AlN buffer structures with alternating high and low V/III ratios grown by MOCVD," *CrystEngComm*, vol. 18, no. 47, pp. 5152–5159, Nov. 2016, doi: 10.1039/C6CE02130A.

[26] A. Knauer, A. Mogilatenko, S. Hagedorn, J. Enslin, T. Wernicke, M. Kneissl, and M. Weyers, "Correlation of sapphire off-cut and reduction of defect density in MOVPE grown AlN," *Phys. Status Solidi B*, vol. 253, no. 5, pp. 809–814, Mar. 2016, doi: 10.1002/pssb.201600075.

[27] M. A. Moram and M. E. Vickers, "X-ray diffraction of III-nitrides," *Rep. Prog. Phys.*, vol. 72, no. 3, p. 036502, Dec. 2008, doi: 10.1088/0034-4885/72/3/036502.

[28] A. Fontserè, A. Pérez-Tomás, M. Placidi, P. Fernández-Martínez, N. Baron, S. Chenot, Y. Cordier, J. C. Moreno, P. M. Gammon, and M. R. Jennings, "Temperature dependence of Al/Ti-based Ohmic contact to GaN devices: HEMT and MOSFET," *Microelectron. Eng.*, vol. 88, no. 10, pp. 3140–3144, Oct. 2011, doi: 10.1016/j.mee.2011.06.015.

[29] M. Dutta, F. Koeck, R. Hathwar, S. Goodnick, R. Nemanich, and S. Chowdhury, "Demonstration of diamond-based Schottky p-i-n diode with blocking voltage > 500 V," *IEEE Electron Device Lett.*, vol. 37, no. 9, pp. 1170–1173, Sep. 2016, doi: 10.1109/LED.2016.2592500.

[30] M. Dutta, F. Koeck, W. Li, R. Nemanich, and S. Chowdhury, "High voltage diodes in diamond using (100) and (111) substrates," *IEEE Electron Device Lett.*, vol. 38, no. 5, pp. 600–603, May 2017, doi: 10.1109/LED.2017.2681058.

[31] F. Iucolano, F. Roccaforte, F. Giannazzo, and V. Raineri, "Barrier inhomogeneity and electrical properties of Pt/GaN Schottky contacts," *J. Appl. Phys.*, vol. 102, no. 11, p. 113701, Dec. 2007, doi: 10.1063/1.2817647.